Control of c-axis orientation of L10-FePd in dual-phase-equilibrium FePd/Fe thin films

T. Ichitsubo, S. Takashima, E. Matsubara, S. Tsukimoto, Y. Tamada et al.

Citation: J. Appl. Phys. **109**, 033513 (2011); doi: 10.1063/1.3544466
View online: http://dx.doi.org/10.1063/1.3544466
View Table of Contents: http://jap.aip.org/resource/1/JAPIAU/v109/i3
Published by the American Institute of Physics.

Control of *c*-axis orientation of $L1_0$-FePd in dual-phase-equilibrium FePd/Fe thin films

T. Ichitsubo,[1,a)] S. Takashima,[1] E. Matsubara,[1] S. Tsukimoto,[2] Y. Tamada,[3] and T. Ono[3]
[1]*Department of Materials Science and Engineering, Kyoto University, Kyoto 606-8501, Japan*
[2]*World Premier International Research Center, Advanced Institute for Materials Research, Tohoku University, Sendai 980-8577, Japan*
[3]*Division of Materials Chemistry, Institute for Chemical Research, Kyoto University, Uji, Kyoto 611-0011, Japan*

(Received 18 September 2010; accepted 10 December 2010; published online 3 February 2011)

This work establishes a method of controlling the *c*-axis-oriented structure of α-Fe (soft magnetic)/$L1_0$-FePd (hard magnetic) thin films in the dual-phase compositional region in thermal equilibrium. Two types of thin films were prepared; one is a single-layered thin film, and the other is a multilayered film, $[\mathrm{FePd}(x\ \mathrm{nm})/\mathrm{Fe}(5\ \mathrm{nm})]_n$ (x: thickness, n: the number of multilayers), both of which are deposited on silica glass substrates. For single-layered films, the ordering process is retarded by phase separation that requires long-range diffusion. In this case, the $\langle 111 \rangle$ oriented domains preferentially grow from the film surface, and the *c*-axis-oriented structure is not obtained. On the contrary, for multilayered films, each FePd layer can undergo ordering without phase separation subject to the constraint of strong biaxial tensile stress resulting from the difference in the thermal contractions between Fe/FePd film and the silica glass substrate. Consequently, the $L1_0$ domains with *c*-axis orientation in the normal direction of the film surface are preferentially formed in the initial amorphouslike structure, eventually leading to the desired *c*-axis-oriented structure.
 [doi:10.1063/1.3544466]

I. INTRODUCTION

Ferromagnetic $L1_0$ ordered alloys FePt, CoPt, and FePd, are under extensive investigation for practical use in perpendicular recording media,[1–10] owing to their significantly large uniaxial magnetocrystalline anisotropy ($K \sim 10^6\ \mathrm{J/m^3}$), where the *c*-axis is the easy axis of magnetization.[11] The large anisotropy can reduce the size of magnetic nanoparticles down to several nanometers without exhibiting superparamagnetic behavior in terms of the KV/k_BT criterion (V is the volume of magnetic particles, T is the temperature, and k_B is the Boltzmann constant). However, for applications to magnetic recording media, we require well-ordered $L1_0$ particles with their *c*-axis oriented in the normal direction in the thin films.

Recently, a method to synthesize fully ordered FePt nanoparticles has been reported;[8–10] in this method, high-melting-temperature SiO_2 covers the surface of isolated FePt nanoparticles prepared by Sun's method,[1] and subsequently the SiO_2-covered nanoparticles are annealed at sufficiently high temperature for fully ordering reaction to extract their high coercivity. On the other hand, one can choose an epitaxial-like growth method by utilizing an appropriate substrate as a method of controlling the *c*-axis orientation of $L1_0$ ordered alloys.[3–6] It has also been claimed that the difference in the thermal expansion coefficients between FePt or CoPt and the substrate plays a significant role in the *c*-axis orientation of $L1_0$ alloys.[4–7] In addition, it has been shown that the *c*-axis of FePt is oriented in the normal direction of the film surface with the aid of B_2O_3 interlayers,[12,13] and some of the present authors have tried to elucidate the mechanism of how the *c*-axis orientation of FePt or CoPt occurs with the B_2O_3 interlayers.[14] According this work, the biaxial-strain field due to the difference in the thermal contraction plays a significant role in making *c*-axis aligned in the normal direction of the thin films; this can be regarded as one of the effects of applying an external field.[15–18]

A well-known problem raised recently is that the switching magnetic field is still too high for write applications due to the high anisotropy field caused by the large K. In order to ameliorate this condition, a composite of soft and hard magnetic materials is effective in reducing the switching field.[19,20] As a model case, we have recently reported the exchange-coupling magnetic property of the α-Fe/$L1_0$-FePd dual-phase region in the Fe–Pd alloy system,[21] and Schied *et al.*[22] also reported recently the exchange-coupling behavior of this same system. The Fe–Pd alloy system is attractive in that the soft magnetic α-Fe and hard magnetic $L1_0$-FePd coexist in thermal equilibrium. The intention of this work is to establish the method of controlling the *c*-axis orientation of $L1_0$ ordered domains in the dual-phase region in Fe–Pd alloy system.

II. EXPERIMENTAL

Thin films were deposited on SiO_2 glass substrates by using a three-cathode magnetron sputtering apparatus with 2-in.-diameter Fe and Pd targets; rf (13.56 MHz) sputter depositions were performed at room temperature in an Ar (purity: 99.99%) atmosphere of about 0.3 Pa, after the base pressure reached about 10^{-5} Pa. The distance between the

a)Electronic mail: tichi@mtl.kyoto-u.ac.jp.

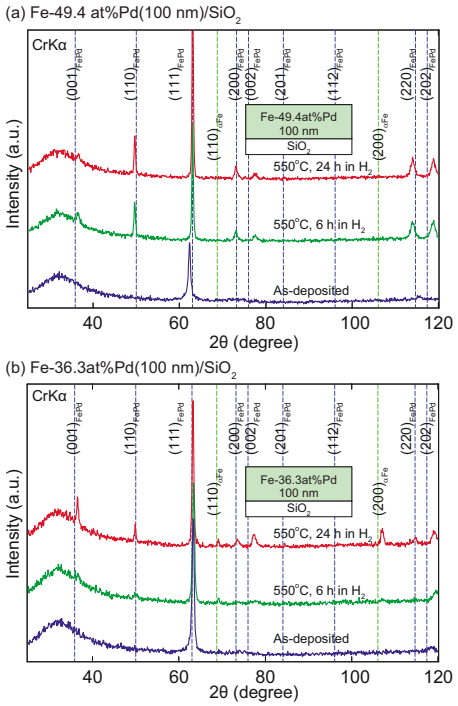

FIG. 1. (Color online) XRD profiles obtained for the single-layered thin films of two compositions: (a) Fe−49.4 at. %Pd and (b) Fe−36.3 at. %Pd. The annealing treatments were done at 550 °C for 6 and 24 h. The former composition is in the single phase region, and the latter is in the dual phase (Fe/FePd) region. The dashed lines are also drawn referring to each powder diffraction file, Fe: #06–0696 and $L1_0$-FePd: #02–1440.

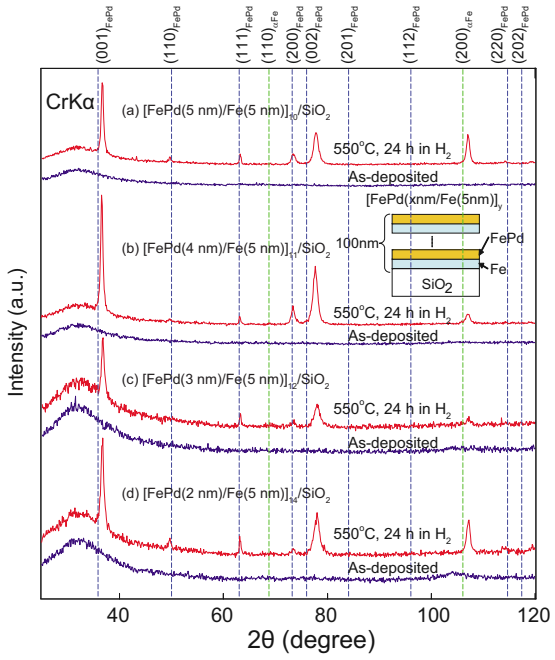

FIG. 2. (Color online) XRD profiles obtained after annealing at 550 °C for 24 h, for multilayered thin films, (a) $[FePd(5\ nm)/Fe(5\ nm)]_{10}$, (b) $[FePd(4\ nm)/Fe(5\ nm)]_{11}$, (c) $[FePd(3\ nm)/Fe(5\ nm)]_{12}$, and (d) $[FePd(2\ nm)/Fe(5\ nm)]_{14}$ on SiO_2-glass substrates.

cathodes and a rotating substrate was set at 200 mm (as long as possible) to maintain surface flatness and compositional homogeneity.

We have prepared following two types of thin films: single-layered thin films and multilayered thin films. In both types of films, the overall thicknesses were about 100 nm. For the single-layered thin films, cosputtering of Fe and Pd were performed simultaneously so as to obtain the objective compositions. For the multilayered thin films, first several nanometers of Fe was sputtered, followed by several nanometers of Fe−50 at. %Pd deposited by co-sputtering, and these procedures were repeated until the total film thickness reached about 100 nm. After the depositions, to attain a fully ordered structure of FePd without oxidation, the thin films were annealed at 550 °C for 6 and 24 h under H_2 gas flow.

The crystallographic orientation of the post-annealed thin films was analyzed by the θ-2θ x-ray diffraction (XRD) method using Cr $K\alpha$ radiation and the surface topographic morphology and the composition of the films were observed and measured by field emission scanning electron microscope (FE-SEM) with the energy dispersion x-ray spectrometer and transmission electron microscope (TEM). A superconducting quantum interference device (Quantum Design) with a field of up to 30 kOe (3 T) was used to measure the hysteresis curves at room temperature.

III. RESULTS

Figure 1 shows the XRD profiles obtained for the single-layered thin films of two compositions; (a) Fe−49.4 at. %Pd is in the single $L1_0$ phase region and (b) Fe−36.3 at. %Pd is in the dual phase (Fe/FePd) region. In the as-deposited films of both compositions, the ⟨111⟩ axis is strongly oriented along the normal direction of the film surface. After annealing at 550 °C for 6 and 24 h, in Fe−49.4 at. %Pd the other peaks (e.g., 200, 002 peaks) appear but in Fe−36.3 at. %Pd the other peaks are invisible after annealing for 6 h but appear after annealing for 24 h. This is because only ordering processes allowed by short range diffusion occur in the former case, whereas phase separation by long range diffusion is required for the latter case. As a result, the ordering is retarded in the dual-phase compositional region and not in the single-phase compositional region. We also checked that this trend was more prominent for bulk samples of the similar compositions (not presented here). Interestingly, in both cases, the 002 peak position is at a higher angle than that in the powder diffraction file (PDF#02–1440) for $L1_0$-FePd. From this result, we find that the oriented $L1_0$ domains have a smaller c-axis than usual, which is due to the stress effect (this is discussed later).

In contrast, the XRD profiles for the multilayered thin films are totally different from the single-layered thin films. As shown in Fig. 2, we cannot see any peaks except the halo peak from the SiO_2 glass in all the as-deposited films, indicating that their structure is an amorphouslike structure or aggregation of tiny small crystals. After annealing at 550 °C for 24 h, however, the diffraction peaks from the $L1_0$ ordered domains appear. It is here noted that 001 and 002 peaks are very prominent in comparison to the other 110, 111, and 200 peaks, which clearly indicate that the c-axis of $L1_0$ domains are almost aligned in the normal direction of the film surface in all films. Furthermore, we note that the 200 peak from α-Fe is also strong, while the 110 peak (the strongest line) is almost invisible. That is, it may be suggested that the c-axis

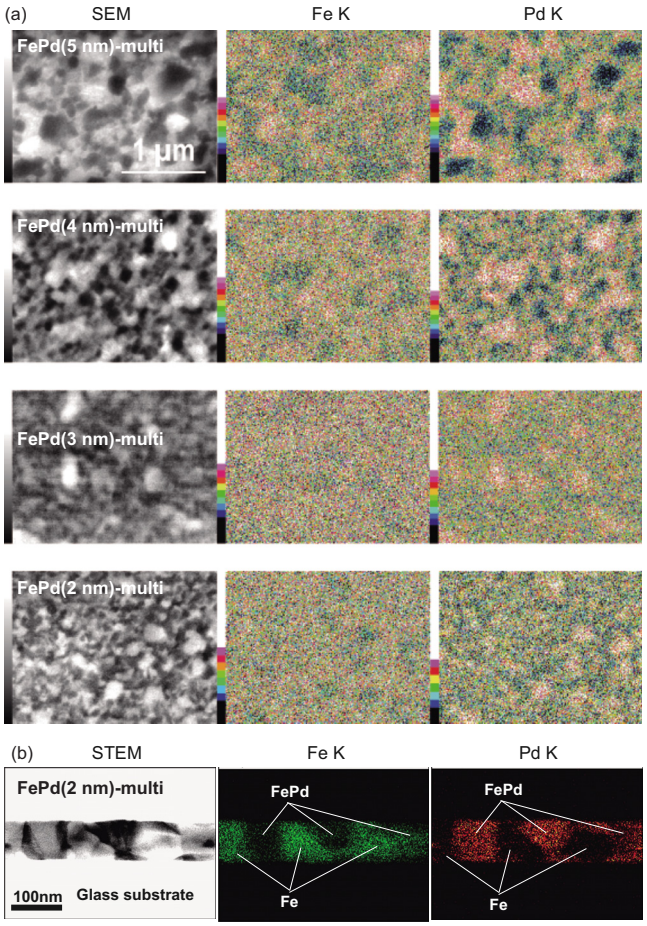

FIG. 3. (Color online) (a) FE-SEM microstructure and composition mappings of Fe and Pd for each multilayered thin film and (b) the cross-section TEM micrograph and composition mappings of $[\mathrm{FePd}(2\ \mathrm{nm})/\mathrm{Fe}(5\ \mathrm{nm})]_{14}/\mathrm{SiO_2}$ film. The denotations, "FePd 5 nm," "FePd 2 nm," etc., mean $[\mathrm{FePd}(5\ \mathrm{nm})/\mathrm{Fe}(5\ \mathrm{nm})]_{10}$, $[\mathrm{FePd}(2\ \mathrm{nm})/\mathrm{Fe}(5\ \mathrm{nm})]_{14}$, etc.

of $L1_0$ domains are cooperatively/simultaneously aligned with the 200 axis of α-Fe. Figure 3(a) shows the FE-SEM microstructure and composition mappings of Fe and Pd for each multilayered thin film and Fig. 3(b) shows the cross-section TEM micrograph of $[\mathrm{FePd}(2\ \mathrm{nm})/\mathrm{Fe}(5\ \mathrm{nm})]_{14}/\mathrm{SiO_2}$ film. These figures show that the Pd-rich, i.e., FePd, regions are embedded in the Fe matrix; the size of the FePd regions in the FE-SEM micrographs are about 100 nm in all cases, which is consistent with the size evaluated by TEM cross-section and mapping micrographs. It is also found that the FePd domains are coarsened after annealing the multilayered thin films, even though the films are initially fabricated by alternate deposition of each layer.

Figure 4 shows the magnetization-field (M-H) curves obtained for single-layered thin films (upper two figures) and multilayered thin films (lower two figures). In Fe−49.4 at. %Pd single-layered thin film, the coercivity H_c is over 2 kOe and little magnetic anisotropy is present. However, in Fe−36.3 at. %Pd single-layered thin film, a small amount of magnetic anisotropy can be seen, which is due to the fact that the peak intensity of the 002 peak is higher than that of the 200 peak in Fe−36.3 at. %Pd (although the overall degree of the 001 orientation is low). In contrast, the magnetic anisotropy can be clearly seen in the multilayered thin films; the "out-of-plane" coercivity $H_{c\perp}$ is twice or three times as large as the "in-plane" coercivity $H_{c\parallel}$. These magnetic anisotropic properties are definitely caused by the c-axis of $L1_0$ domains being well-oriented in the multilayered thin films, as shown in Fig. 2. However, the slopes of the M-H curves for "out-of-plane" are lower than those for "in-plane," indicating that the overall film behaves like a planar magnetic substance (for both phases are ferromagnetic), equivalently, the lower slopes of the "out-of-plane" M-H curves results from demagnetizing effects. Since $K > 2\pi M^2$ for the $L1_0$ FePd alloy, this demagnetization effect mainly comes from the soft magnetic Fe.

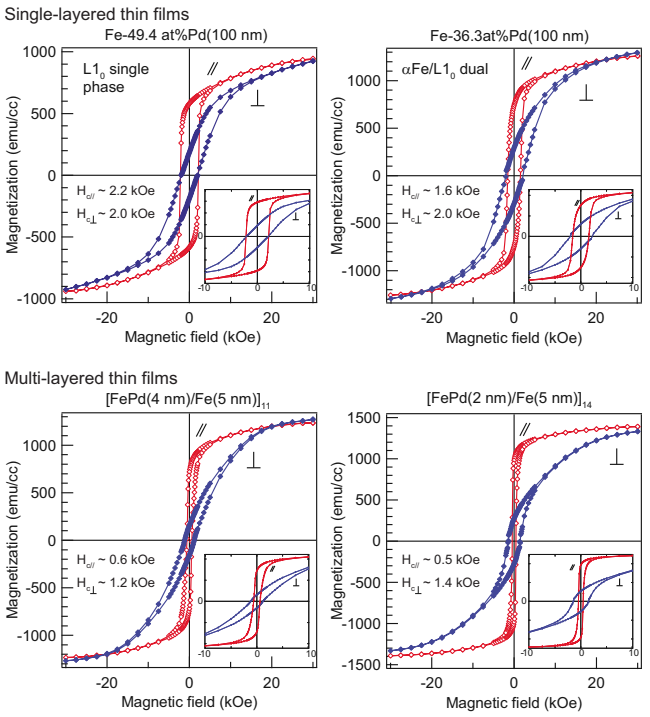

FIG. 4. (Color online) The magnetization-field (M-H) curves obtained for single-layered thin films (upper two figures) and multilayered thin films (lower two figures). The insets magnify the curves around the origin. The smybols ∥ and ⊥ mean, respectively, "in-plane" and "out-of-plane" directions of applying the magnetic field during the M-H curve measurement.

IV. DISCUSSION

Figure 5(a) summarizes the degree of the 001 orientation, which was roughly evaluated by the Lotgering method.[23] According to the method, the degree of orientation F associated with the [001] direction is defined as

$$F_{001} = (p - p_0)/(1 - p_0), \tag{1}$$

where p is the value of the XRD intensity ratio, given by $\Sigma I(00l)/\Sigma I(\mathrm{hkl})$, and p_0 is the value for the perfectly random orientation. This figure also shows the additional results for the other single-layered thin films; Fe−54.2 at. %Pd and Fe−6.0 at. %Pd. In the single-layered thin films, the degrees of 001 orientation, F_{001}, are around 0 (except for Fe−6.0 at. %Pd), whereas F_{001} in each multilayered thin film is quite high (about 0.8). Thus, the c-axis orientation can

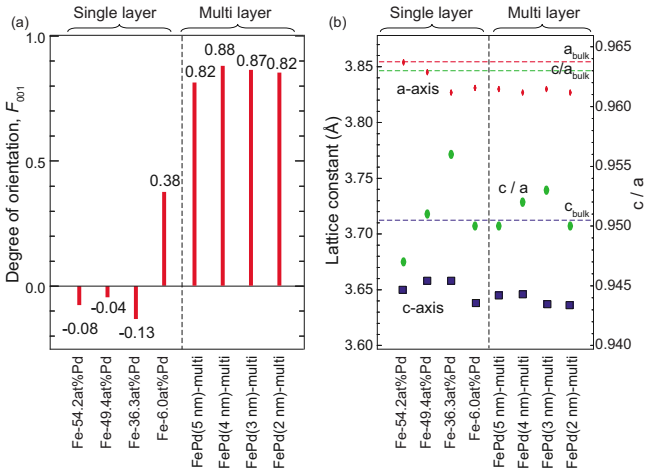

FIG. 5. (Color online) (a) The degree of orientation associated with the 001 axis, evaluated by the Lotgering method (Ref. 23). (b) The axial ratio of the $L1_0$-ordered FePd in the thin films used in the present experiments. The denotations "FePd(5 nm)-multi," etc., means the $[\text{FePd(5 nm)/Fe(5 nm)}]_{10}/\text{SiO}_2$. The dashed lines are the values of the bulk sample of Fe–50.6 at. %Pd.

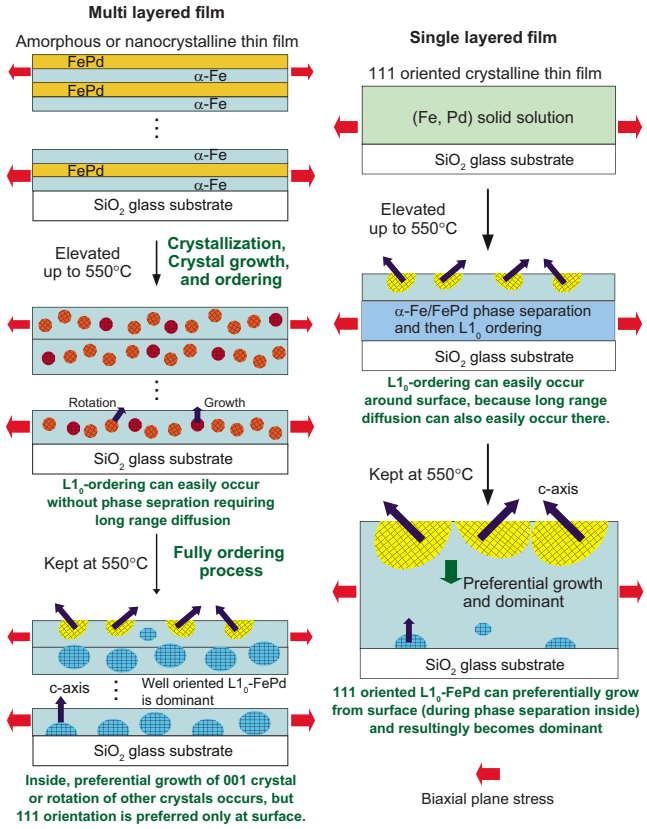

FIG. 6. (Color online) Schematic illustration showing the ordering and phase separation processes under the biaxial tensile stress for multilayered thin films and single-layered thin films. Based on the experimental axial ratio, the biaxial stress is evaluated to be about 700 MPa.

be markedly observed in the multilayered thin films, although this is not the case for the single-layered thin films.

We now consider why such high degrees of the c-axis orientation are realized in the multilayered thin films. Figure 5(b) show the lattice parameters, a and c-axes, and the axial ratio c/a of the $L1_0$ FePd domains embedded in the films. The values of the bulk materials are also shown for comparison. As found from this figure, the a-axis lattice parameter is not so different from the value of the bulk sample but the c-axis lattice parameter is much lower than the bulk value; resulting, the axial ratio c/a is also very low. These values are evaluated by the 200 peak for a-axis and the 002 and 001 peaks for c-axis. Since we employed θ-2θ method in XRD, the crystallographic planes of the crystallites associated with the diffraction are always parallel to the film surface. Therefore, the c parameter evaluated by this method is associated with the crystallites whose c-axes are oriented in the normal direction, and the-axis of the $L1_0$ domains oriented in the normal direction is considerably contracted in all the films.

This lowering of the c-axis or c/a can be understood by the internal (residual) stress that would be caused by the difference in the thermal contraction between FePd–Fe and a SiO_2 glass substrate. During sputter-deposition, the substrate and deposited FePd–Fe are both at high temperature but after deposition they are cooled down to room temperature. In this cooling process, the FePd–Fe alloy is considered to shrink more than the SiO_2 glass substrate because the thermal expansion coefficient silica glass is quite low (of the order 10^{-7} 1/K). Thus, the FePd/Fe films are subjected to biaxial tensile stress because they are under a plane-stress condition.

Based on our previous paper,[14] let us estimate a magnitude of such a biaxial tensile stress that is applied to the FePd domains embedded in the thin film. Here the experimental axial ratio is expressed as $(c/a)_{\text{exp}}$, and the tetragonal distortion in a stress-free "equilibrium" state (which is measured from the mother fcc-disordered phase) is denoted as $\epsilon^*_{\text{eq}} \approx (1/3)[1-(c/a)_{\text{eq}}]$, where $(c/a)_{\text{eq}}$ is the axial ratio in the stress-free state. Then, the tetragonal distortion is estimated to be $\epsilon^*_{\text{eq}} \approx 0.0123$ by using the axial ratio, $(c/a)_{\text{eq}}=0.963$, of the bulk sample in Fig. 5(b). Under the plane-stress condition (i.e., $\sigma_3=0$), the elastic strain for the in-plane directions ϵ_a is expressed as

$$\epsilon_a = \frac{1-2\epsilon^*_{\text{eq}} - (1+\epsilon^*_{\text{eq}})(c/a)_{\text{exp}}}{(c/a)_{\text{exp}} + 2c_{12}/c_{11}}, \tag{2}$$

and the "in-plane" stresses σ_1 and σ_2 are given by

$$\sigma_1 = \sigma_2 = \frac{c_{11}^2 + c_{11}c_{12} - 2c_{12}^2}{c_{11}}\epsilon_a, \tag{3}$$

where the subscripts 1, 2, and 3 are assigned for the in-plane directions [Eqs. (1) and (2)] and out-of-plane direction [Eq. (3)] of a thin film, and c_{ij} denote the elastic constants of FePd. Tentatively, we assume that the elastic constants of ordered and disordered FePd are equal to the single-crystal elastic constants of an fcc disordered FePd.[24] Since $(c/a)_{\text{exp}}$ is approximately 0.951 as shown in Fig. 5(b), the in-plane stresses are estimated to be $\sigma_1=\sigma_2 \approx 700$ [MPa]. Thus, the experimental low c/a ratio indicates that considerably large tensile stresses are being applied to the FePd domains in the films.

Based on the biaxial tensile stress discussed above, we address the c-axis orientation mechanism in the FePd/Fe films. Figure 6 illustrates the ordering and phase-separation process under the biaxial tensile stress applied to the film for

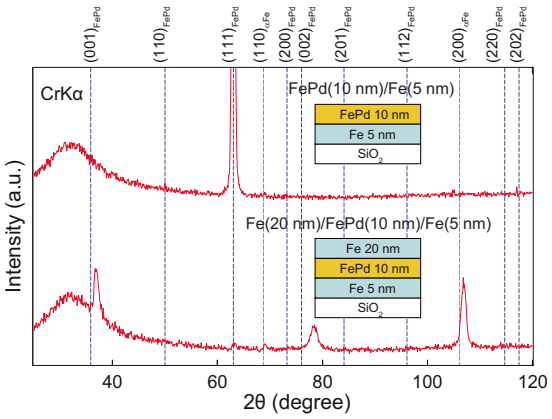

FIG. 7. (Color online) XRD profiles obtained after annealing the two films, FePd(10 nm)/Fe(5 nm)SiO_2 and Fe(20 nm)/FePd(10 nm)/Fe(5 nm)SiO_2, at 550 °C for 24 h.

both single and multilayered thin films. In the multilayered thin film case, long range diffusion is not required because each FePd layer satisfies the compositional requirement (for two phases are originally separated in the as-deposited stage for the multilayered films) so that it can easily undergo only ordering. In contrast, single-layered thin films need long range diffusion for phase separation to occur. For multilayered thin films under the biaxial tensile stress, *c*-axis-oriented domains are preferentially formed in each layer, except in the vicinity of the surface (because the ⟨111⟩-oriented domains would be favorable there in terms of reducing the surface energy and releasing the elastic stress). Thus, *c*-axis-oriented FePd domains are likely to be formed or chosen from the tiny small crystals owing to the biaxial tensile stress in the multilayered thin film. On the contrary, this situation is thoroughly different for single-layered thin films. As mentioned above, this system (i.e., of Fe-rich composition in the Fe–Pd alloy system) requires phase separation with long range diffusion, in addition to the ordering process. In terms of diffusion, long range diffusion, and therefore ordering and phase separation, can take place relatively easily in the vicinity of the surface, whereas their kinetics would be retarded inside the film. Near the surface the ⟨111⟩-oriented ordered domains are considered to preferentially grow, because the surface energy can be reduced by the formation of the ⟨111⟩-oriented domains. Moreover, as seen in Fig. 1, the as-deposited single-layered thin film already contains the ⟨111⟩-oriented crystallites. It seems to be quite difficult to orient the *c*-axis in the normal direction of the film surface, when the ⟨111⟩-oriented structure is initially formed before annealing.

To ensure the validity of the mechanism described above, we have performed one additional experiment by preparing the two samples; one is a two-layer film whose upper layer is just FePd without any cover (bottom layer is an Fe layer), and the other is a three-layered film, where the top layer is a relatively thick (20 nm) Fe layer. Figure 7 shows the XRD profiles after annealing at 550 °C for 24 h. The ⟨111⟩-oriented structure is formed in the two-layer film, whereas the *c*-axis is completely oriented in the normal direction for the three-layer film. The most important condition to attain a complete *c*-axis-oriented structure is to prohibit the ordering reaction from the surface, and to effectively exploit the biaxial stress. The latter *c*-axis-oriented film exhibit the intriguing spring magnetic behavior due to the exchange coupling between hard $L1_0$-FePd and soft α-Fe.[21]

V. CONCLUSIONS

In conclusion, we have devoted this work to the investigation of the *c*-axis-oriented structure formation of FePd/Fe thin film in the dual phase region in thermal equilibrium, and have reached several conclusions. First, in the dual phase region, phase separation with long range diffusion is required in addition to the ordering kinetics to attain thermal equilibrium during annealing. Second, in the multilayered thin films, the ordering in each layer easily occurs without long range diffusion under the constraint of a strong biaxial tensile stress. Consequently, the *c*-axis-oriented FePd domains are preferentially formed or chosen from many tiny crystals, and they eventually become dominant. On the contrary, in the single-layered thin films, the ordering process itself is retarded by the indispensable phase separation accompanied by long-range diffusion. In this case, the ⟨111⟩-oriented domains tend to grow preferentially near the surface in terms of reducing the surface energy and releasing the elastic energy. Consequently, the *c*-axis-oriented structure cannot be attained for the single-layered thin films. Finally, to attain control of the *c*-axis orientation in $L1_0$ ordered alloys, the residual biaxial tensile stress must be effectively exploited, the ⟨111⟩-oriented crystals should be reduced as low as possible in the as-deposited film, and the ordering process must be prohibited from occurring at the surface of the film.

ACKNOWLEDGMENT

This work was partly supported by a Grant-in-Aid for "Wakate Kenkyu A (20686043)" from the Japanese Society for the Promotion of Science (JSPS). One of the authors, T.I., was indeed grateful to Ms. Niedziela and Jennifer Lynn, for reading and correcting our manuscript.

[1]S. Sun, C. B. Murray, D. Weller, L. Folks, and A. Moser, Science **287**, 1989 (2000).
[2]D. H. Ping, M. Ohnuma, K. Hono, M. Watanabe, T. Iwasa, and T. Masumoto, J. Appl. Phys. **90**, 4708 (2001).
[3]T. Shima, K. Takanashi, Y. K. Takahashi, and K. Hono, Appl. Phys. Lett. **85**, 2571 (2004).
[4]D. Halley, B. Gilles, P. Bayle-Guillemaud, R. Arenal, A. Marty, G. Patrat, and Y. Samson, Phys. Rev. B **70**, 174437 (2004).
[5]O. Ersen, V. Parasote, V. Pierron-Bohnes, M. C. Cadeville, and C. Ulhaq-Bouillet, J. Appl. Phys. **93**, 2987 (2003).
[6]M. Abes, O. Ersen, C. Meny, G. Schmerber, M. Acosta, J. Arabski, C. Ulhaq-Bouillet, A. Dinia, P. Panissod, and V. Pierron-Bohnes, J. Appl. Phys. **101**, 063911 (2007).
[7]P. Rasmussen, X. Rui, and J. E. Shield, Appl. Phys. Lett. **86**, 191915 (2005).
[8]S. Yamamoto, Y. Morimoto, T. Ono, and M. Takano, Appl. Phys. Lett. **87**, 032503 (2005).
[9]Y. Tamada, S. Yamamoto, S. Nasu, and T. Ono, Phys. Rev. B **78**, 214428 (2008).
[10]Y. Tamada, S. Yamamoto, S. Nasu, and T. Ono, Appl. Phys. Express **2**, 123001 (2009).
[11]T. Klemmer, D. Hoydick, H. Okumura, B. Zhang, and W. A. Soffa, Scr. Metall. Mater. **33**, 1793 (1995).
[12]C. P. Luo, S. H. Liou, L. Gao, Y. Liu, and D. J. Sellmyer, Appl. Phys. Lett.

77, 2225 (2000).
[13]M. L. Yan, H. Zeng, N. Powers, and D. J. Sellmyer, J. Appl. Phys. **91**, 8471 (2002).
[14]T. Ichitsubo, S. Tojo, T. Uchihara, E. Matsubara, A. Fujita, K. Takahashi, and K. Watanabe, Phys. Rev. B **77**, 094114 (2008).
[15]K. Tanaka, T. Ichitsubo, M. Amano, M. Koiwa, and K. Watanabe, Mater. Trans., JIM **41**, 917 (2000).
[16]T. Ichitsubo, M. Nakamoto, K. Tanaka, and M. Koiwa, Mater. Trans., JIM **39**, 24 (1998).
[17]T. Ichitsubo, K. Tanaka, M. Koiwa, and Y. Yamazaki, Phys. Rev. B **62**, 5435 (2000).
[18]K. Tanaka, T. Ichitsubo, and M. Koiwa, Mater. Sci. Eng., A **312**, 118 (2001).
[19]R. H. Victora and X. Shen, IEEE Trans. Magn. **41**, 537 (2005).
[20]D. Suess, J. Lee, J. Filder, and T. Schrefl, J. Magn. Magn. Mater. **321**, 545 (2009).
[21]T. Ichitsubo, S. Takashima, E. Matsubara, Y. Tamada, and T. Ono, Appl. Phys. Lett. **97**, 182508 (2010).
[22]T. Schied, A. Lotnyk, C. Zamponi, L. Kienle, J. Buschbeck, M. Weisheit, B. Holzapfel, L. Schultz, and S. Fäler, J. Appl. Phys. **108**, 033902 (2010).
[23]F. K. Lotgering, J. Inorg. Nucl. Chem. **9**, 113 (1959).
[24]T. Ichitsubo and K. Tanaka, J. Appl. Phys. **96**, 6220 (2004).